

Original Research Article

Theoretical studies of 2-[(E)-(3-phenylmethoxyphenyl)methylideneamino]guanidine as promising drugs against SARS-coronavirus spike glycoproteins by molecular docking combined with molecular dynamics simulation and MM/GBSA calculation

Emmanuel Israel Edache^{1,*}, Adamu Uzairu², Paul Andrew Mamza², Gideon Adamu Shallangwa²

¹Department of Pure and Applied Chemistry, Faculty of Science, University of Maiduguri, P.M.B. 1069, Maiduguri, Borno State, Nigeria

²Department of Chemistry, Faculty of Physical Sciences, Ahmadu Bello University, P.M.B. 1044, Zaria, Kaduna State, Nigeria

ARTICLE INFO

Article history

Submitted: 2022-11-13

Revised: 2023-01-02

Accepted: 2023-03-02

Available online: 2023-03-04

Manuscript ID: PCBR-2211-1237

DOI: 10.22034/pcbr.2023.370115.1237

KEYWORDS

SARS-coronavirus-2

Iminoguanidine

Docking

Molecular dynamics

ADMET

ABSTRACT

The novel 2-[(E)-(3-phenylmethoxyphenyl)methylideneamino]guanidine was put forth as a potential anti-SARS-coronavirus-2 candidate targeting the spike glycoprotein following a docking simulation study. When compared with the standard medications (Chloroquine and Ruxolitinib) with a binding score of -4.8 kcal/mol and -7.0 kcal/mol, respectively, 2-[(E)-(3-phenylmethoxyphenyl)methylideneamino]guanidine's computed binding score of -7.2 kcal/mol indicated that it may have promising anti-SARS-coronavirus-2 activity. The accurate binding of 2-[(E)-(3-phenylmethoxyphenyl)methylideneamino]guanidine to the SARS-coronavirus-2 spike glycoprotein through the appropriate dynamic and energetic behaviours over 20 ns was verified by molecular dynamics simulations as well as MM/GBSA studies. Besides that, *in silico* ADME studies demonstrated 2-[(E)-(3-phenylmethoxyphenyl)methylideneamino]guanidine's general safety and drug-likeness. As a result, the outcomes of this survey gave a strong basis for the *in silico* plan and hypothetical investigation of more potent SARS-coronavirus-2 inhibitors.

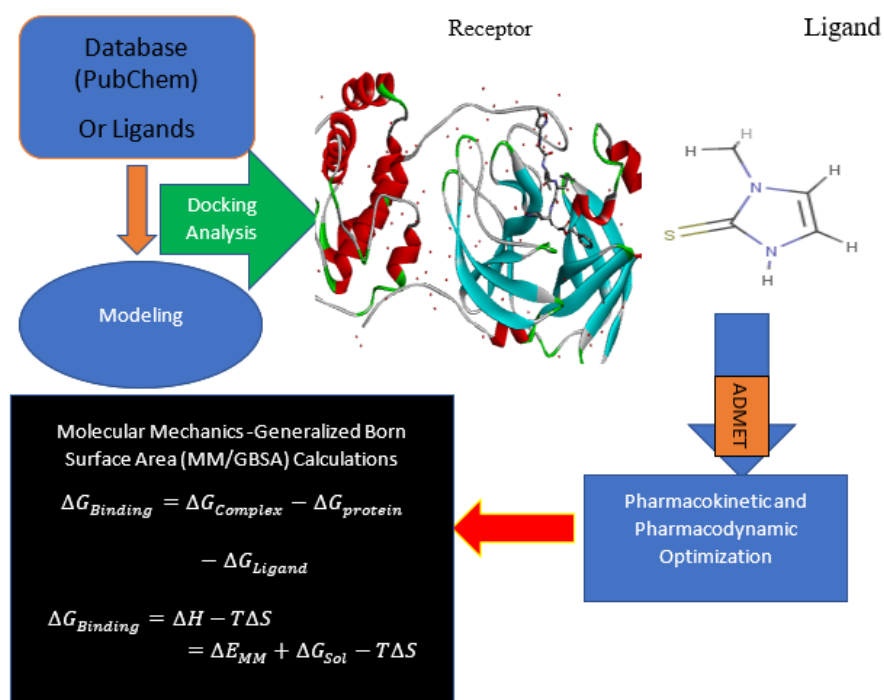
* Corresponding author: Ahmed Mutanabbi Abdula

✉ E-mail: ahm.chem@yahoo.com;

© 2022 by SPC (Sami Publishing Company)



GRAPHICAL ABSTRACT



1- Introduction

Iminoguanidine is an important synthetic class in drug design because of its wide range of pharmacological activity, which includes antibacterial [1,2], antiviral [3], the capacity to distinguish and separate anions from competitive aqueous environments [4], and biomass-based direct air capture [5]. For example, 2-[(E)-(2-bromophenyl)methylideneamino]guanidine was selective for heme oxygenase (HemO) inhibitor [6], 2-[(E)-(2-methoxyphenyl)methylideneamino]guanidine, 2-[(E)-(2-bromophenyl)methylideneamino]guanidine, and 2-[(E)-(4-fluorophenyl)methylideneamino]guanidine acts as an antibacterial activity through the inhibition of *Pseudomonas aeruginosa* [2, 3]. 2-[(E)-(4-fluorophenyl)methylideneamino]guanidine and 2-[(E)-(2-bromophenyl)methylideneamino]guanidine showed a prognosticating anti-SARS-coronavirus nucleoprotein, main protease, and spike glycoproteins activity, respectively [2, 3, 7].

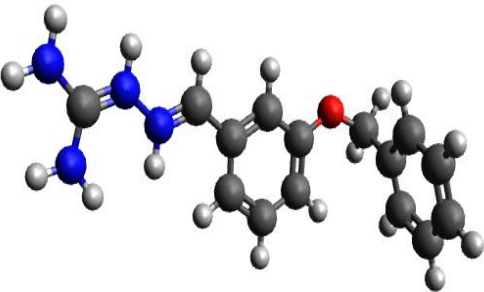
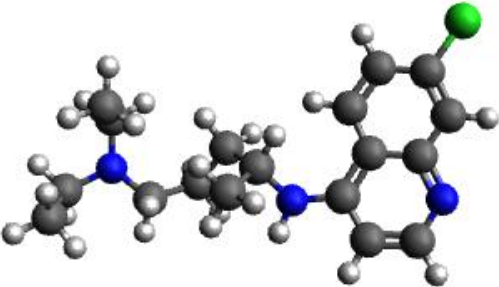
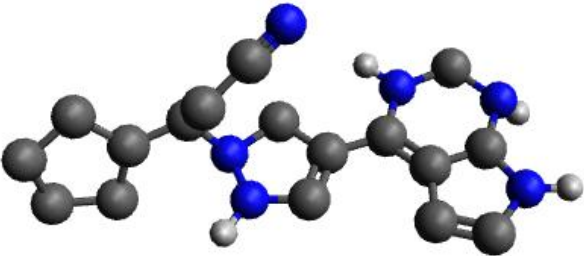
In this research, we present the novel compound 15 also known as “2-[(E)-(4-fluorophenyl)methylideneamino]guanidine” [7], and because of these above facts with the program for the discovery of biologically active compounds, this research involves (i) docking simulation, (ii) “molecular mechanics-generalized Born surface area (MM/GBSA) calculation”, and (iii) we performed *in silico* drug-likeness of 2-[(E)-(4-fluorophenyl)methylideneamino]guanidine against SARS-coronavirus-2 spike glycoproteins. This study describes how small molecular compounds should be selected for drug development in an artificially safe and efficient manner against a target macromolecule. On the other hand, developing and designing drugs in a lab takes a lot of time, money, and effort. Using this *in silico* technique, the drug design for the upcoming class of infectious agents could be improved. The next pandemic may be avoided in large part thanks to this *in silico* strategy.

2- Materials and Methods

The structures of 2-[(E)-(4-fluorophenyl)methylideneamino] guanidine (Table 1) that present studies related to the inhibition of SARS-coronavirus-2 spike glycoprotein (SP) were selected from our previous study [7] to serve as a basis for molecular docking. The 3D structure of the compound including the reference drugs Chloroquine and Ruxolitinib was arranged to

utilize MarvinView Europium.6 and their energies were limited with the Spartan'14 V1.1.4 PM6. Streamlining of energy-limited particles was accomplished using the DFT strategy with B3LYP capability [8,9] and the 6-31G+ fundamental set [10] with the GAUSSIAN 09 bundle [11]. The docking of all the reported molecules in Table 1 was performed using PyRx 0.8 v [12] against SARS-coronavirus-2 SP.

Table 1. Chemical structures and binding affinity of each compound under study.

3D structure	Compound CID	Binding affinity (kcal/mol)
	134130081	-7.2
2-[(E)-(3-phenylmethoxyphenyl)methylideneamino]guanidine <chem>[H]N([H])C(N([H])[H])=[N+](([H])[N+](\ [H])=C\c1cccc(OCc2ccccc2)c1</chem>	2719	-4.8
 Chloroquine <chem>CCN(CC)CCCC(C)NC1=C2C=CC(=CC2=NC=C1)Cl</chem>	25126798	-7.0
 Ruxolitinib <chem>C1CCC(C1)[C@@H](CC#N)N2C=C(C=N2)C3=C4C=CNC4=NC=N3</chem>		

Building of protein 3D structure

The protein structure of spike glycoprotein of SARS-coronavirus-2 (PDB ID: 7MZF) was fetched from the Protein Data Bank. Protein formulation was done by using Auto Dock Tools v1.5.7 [13] and Discovery Studio 2020 Client. The SARS-coronavirus-2 spike glycoprotein (chains A) was chosen for molecular docking production. All water molecules are deleted from the protein before docking. After the water molecules were got rid of, a polar hydrogen atom was added to the protein to ensure proper amino acid ionization and tautomeric states. The structures were docked by the active site defined through a grid box (Vina Search Space = “center_x = -1.5643, center_y = 12.818, center_z = 12.3015”), Dimensions (Angstrom): “size_x = 49.2203297997, size_y = 44.6869613934, size_z = 51.2521103764”, and exhaustiveness = 8.

Molecular dynamics simulations

MD simulations were executed using NAMD v2.14 [14] adopting a 20,000 stages equilibration and 20 ns creation (20 ns at a consistent temperature of 297 K and a steady tension of 1 atm) convention executed in the simulation contents produced by the CHARMM-GUI membrane developer [15]. We employed a timestep of 2 fs. In contrast to our earlier research, the temperature of 310 K was taken into account and saved trajectory frames more frequently, at a frequency of 500 steps. The CHARMM36m force field was used for all calculations. The investigation of MD simulations including estimations of the “root-mean-squared deviation (RMSD) time series, Radius of gyration (RG), Solvent accessible surface area (SASA), and root mean squared fluctuations (RMSF)” were performed using VMD v1.9.3 [16].

Binding free energy calculation

The “molecular mechanics-generalized born surface area (MM/GBSA) approach” [17] and the

MOLAICAL code [18] were used to determine the relative free energies of binding for the most encouraging complex with the spike glycoprotein of SARS-coronavirus-2. The following estimate was made for the MM/GBSA ($\Delta G_{\text{Binding}}$) energy [19]:

$$\Delta G_{\text{Binding}} = \Delta G_{\text{Complex}} - \Delta G_{\text{Protein}} - \Delta G_{\text{Ligand}}$$

$$\Delta G_{\text{Binding}} = \Delta H - T\Delta S = \Delta E_{\text{MM}} + \Delta G_{\text{Sol}} - T\Delta S$$

The terms ΔE_{MM} , ΔG_{Sol} and $T\Delta S$ are “gas phase molecular mechanics, solvation, and conformational entropy”, respectively.

$$\Delta E_{\text{MM}} = \Delta E_{\text{ele}} + \Delta E_{\text{VDW}} + \Delta E_{\text{int}}$$

$$\Delta G_{\text{Sol}} = G_{\text{polar solvation}} + G_{\text{non-polar solvent}} + T\Delta S$$

Where ΔE_{ele} , ΔE_{VDW} , and ΔE_{int} are changes in “electrostatic energies, Van der Waals energies, and internal energies”. The generalized born model and the solvent-accessible surface area (SASA) can be used to calculate the polar and non-polar solvation, respectively. In addition, $T\Delta S$ can be computed using normal mode analysis. In MM/GBSA calculations, the solvent dielectric constant and n constant were assigned the values 78.5 and 0.03012 kJ/mol, respectively.

3- Results and Discussion

By importing our findings into the Discovery Studio 2020 Client, we were able to obtain the 2D and 3D interactions of the binding modes. The amino acids represented in Figures 1 to 3 are those that contribute significantly energetically to the overall binding affinities of interaction in the interactions taking place between the chosen drug compounds and the 3D protein. Most importantly, the relationship of interactions between amino acids and various ligands, including Van der Waals interactions, electrostatic interactions (π -cation), hydrophobic contacts (π -sigma, π -alkyl, and alkyl), and hydrogen bonds (π -donor HB, conventional hydrogen bond, and carbon-

hydrogen bond), can offer information about molecular interactions [20]. The docking results of selected compounds are listed in Table 1. 2-[(E)-(4-fluorophenyl) methylideneamino] guanidine (Figure 8), which is the best-performing molecule in the data set, has the most binding energy (-7.2 kcal/mol). All ligands bind to the active residues in the predetermined catalytic pocket, as demonstrated by the docked conformations. The key residues in the binding catalytic pocket were Trp104, Leu35, Val36, Phe6, Cys4, Leu3, and Asn11. The best compound

“2-[(E)-(4-fluorophenyl)methylideneamino]-guanidine” formed two conventional hydrogen bonds with Asn11 residue, one pi-donor hydrogen bond with Trp104 residue, and show pi-sigma and pi-alkyl bonds with Val35 and Leu36, respectively. These interactions explain the stability of the compound. The binding interactions of the reference drugs (Chloroquine and Ruxolitinib) with receptor 7MZF and their bond distance are shown in Figures 7 and 8, respectively.

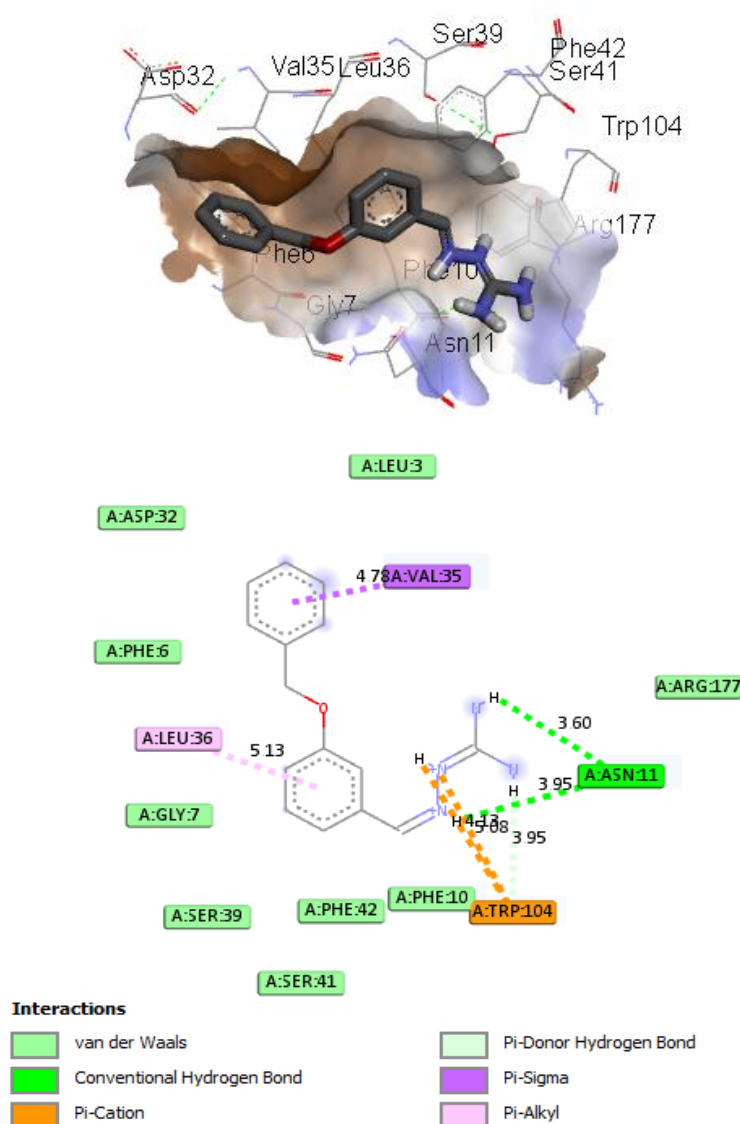


Fig. 1. The active site residues of the 7MZF protein interacting with 2-[(E)-(4-fluorophenyl)methylideneamino]guanidine to identify the active residues of spike glycoprotein.

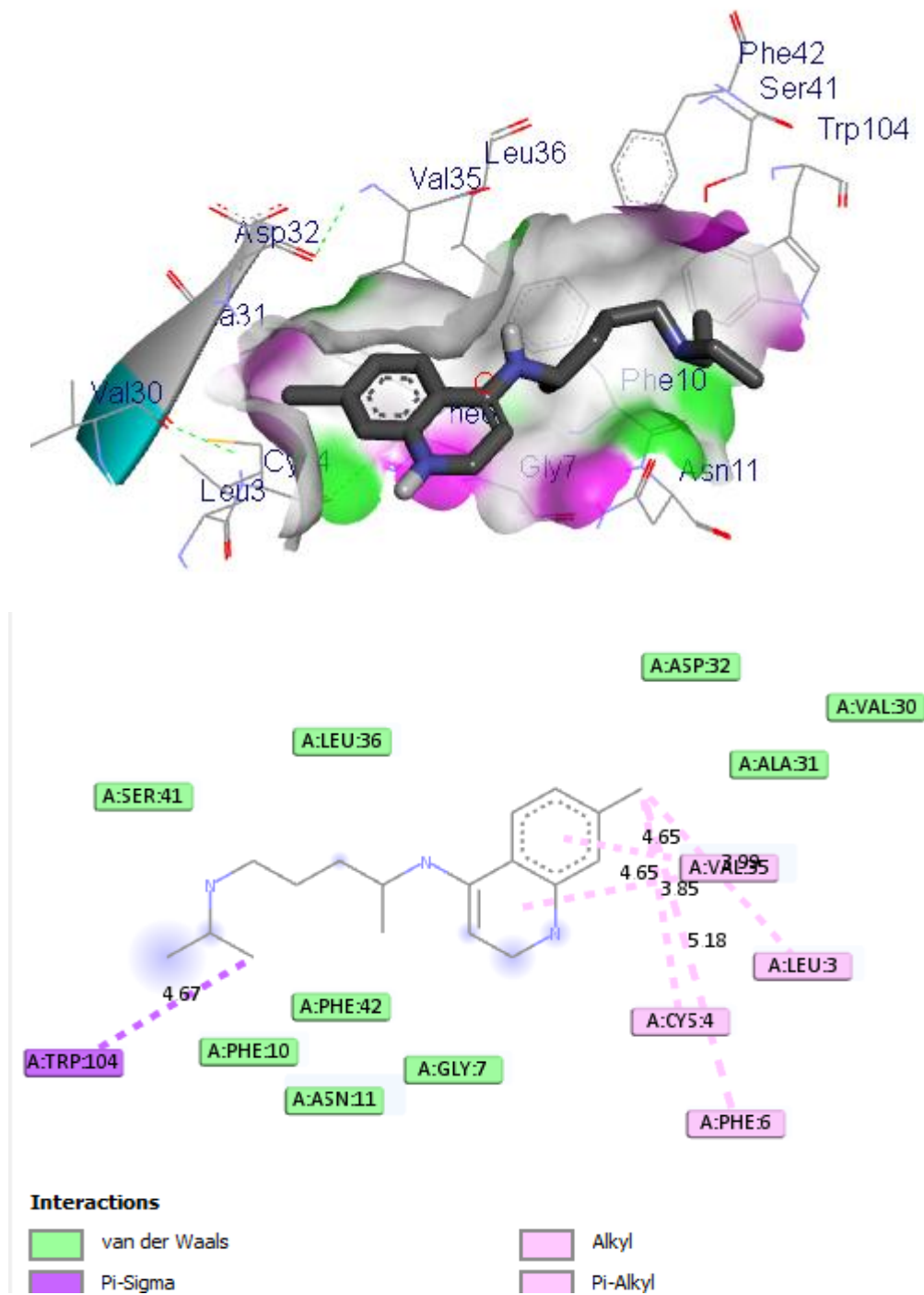


Fig. 2. The active site residues of the 7MZF protein interact with Chloroquine to identify the active residues of spike glycoprotein.

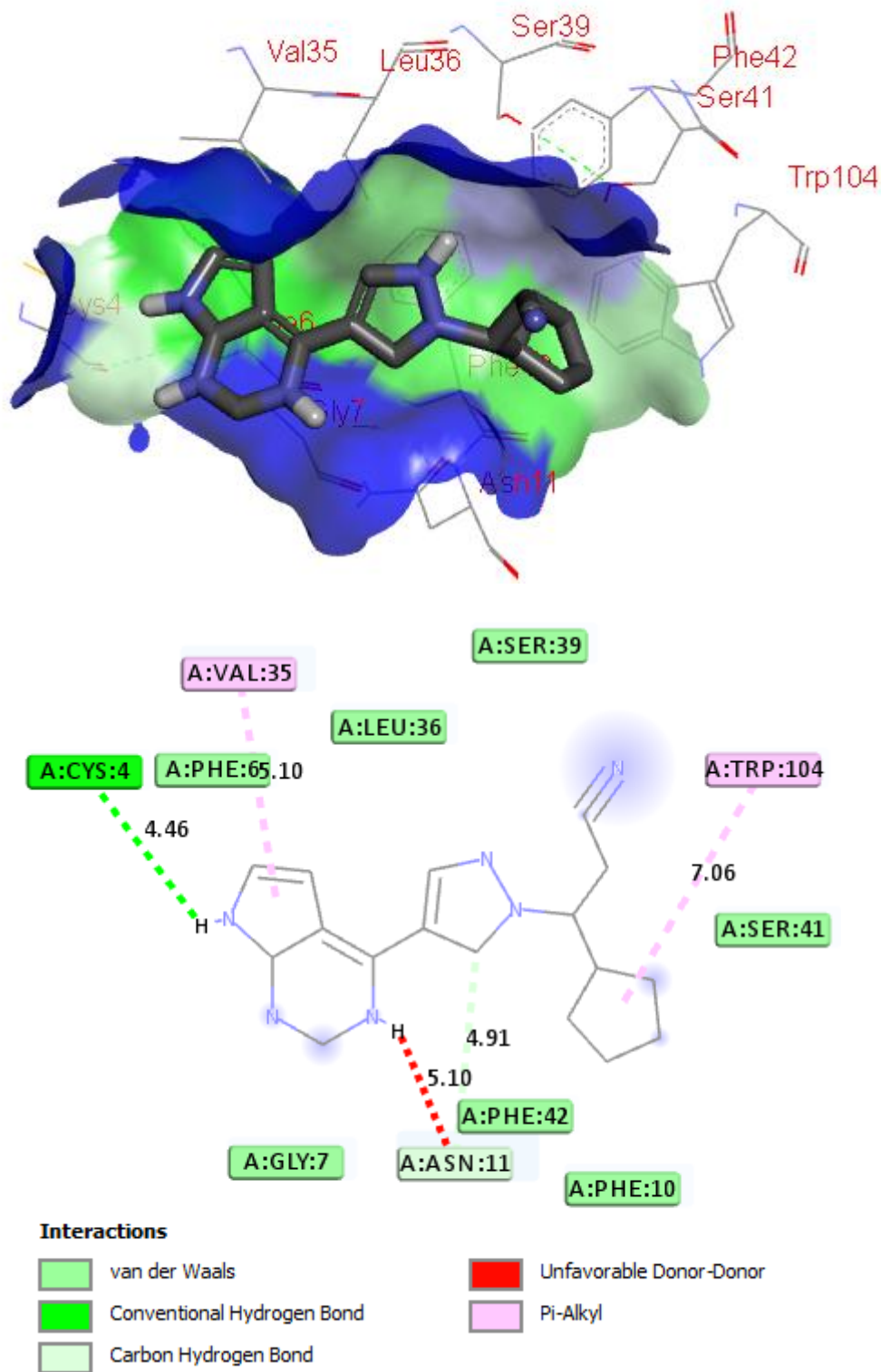


Fig. 3. The active site residues of the 7MZF protein interact with Ruxolitinib to identify the active residues of the spike glycoprotein.

MD simulations

The substance, 2-[(E)-(3-phenylmethoxyphenyl)methylideneamino]guanidine (Figure 4), was seen to form a conventional hydrogen bond with Asn11, Phe10, and Ser41 residues that were at a distance of 3.62, 4.16, 5.52, 5.29, 3.16, and 2.81 long, respectively. Two additional residues, Trp104 at a distance of 3.56 and Gly7 at a distance of 4.32, were seen to be involved in the compound's pi-donor hydrogen bond

interactions. The interactions were increased to more conventional and pi-donor hydrogen bonds, one electrostatic interaction, and no evidence of hydrophobic interactions after running MD simulations for 20 ns. The new conventional hydrogen bonds forming residues were Phe10 and Ser41, pi-donor hydrogen bond with residue Gly7, and electrostatic interactions with residue Phe42 (Figure 4).

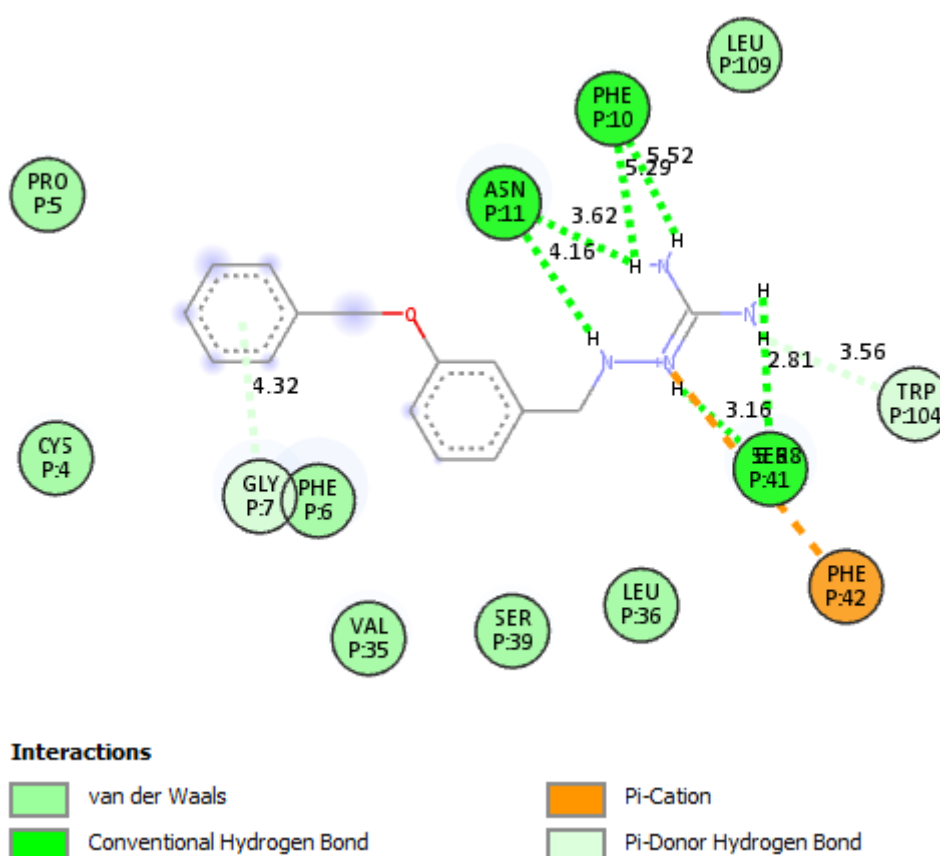


Fig. 4. The 2D representation of 2-[(E)-(3 phenylmethoxyphenyl)methylideneamino]guanidine with the SARS-coronavirus-2 spike glycoprotein (PDB id: 7MZF) after 20 ns MD simulations.

Using root mean square deviation (RMSD) to calculate the scalar spacing between protein and ligand along the trajectory, molecular dynamics were analyzed. The evolution of the representation, root mean square deviation (RMSD), the radius of gyration (RG), and solvent accessible surface area (SASA) over a 20-ns period are depicted in Figure 5. Before

calculating RMSD, all protein frames were already aligned over the reference frame backbone. The average RMSD for backbone atoms in 2-[(E)-(3-phenylmethoxyphenyl)methylideneamino]guanidine (complex) and spike protein (PDB id: 7MZF) were found to be 1.7 Å and 1.09 Å, respectively. The minutely varying number of conventional hydrogen bonds

among amino acids (protein residues) during the molecular dynamic simulations run is what causes the minor fluctuations seen in the RMSD plots (Figure 5A). The 2-[(E)-(3-phenylmethoxyphenyl)methylideneamino]guanidine complex appeared to be more steady during the 20 ns MD simulation, according to the RMSD evaluation of both structures. The average RMSF value for the complex and protein was found to be 0.0554 Å 0.0551 Å, respectively. According to RMSF evaluation, the spike glycoprotein of SARS-coronavirus-2 produced less fluctuation than the binding of 2-[(E)-(3-phenylmethoxyphenyl)methylideneamino] guanidine complex (Figure 5B). A parameter to evaluate the folding of regular alpha helix into a three-dimensional protein structure is the radius of gyration (RG). RG denotes a change in the overall size and compactness of the protein structure. The average RG values for complex and protein were 17.94 Å and 17.87 Å, respectively. According to the RG assessment, there is no appreciable difference in the target protein's compactness of folding after binding (Figure 5C). In contrast, little variations in the complex's RG may have been caused by the 2-[(E)-(3-phenylmethoxyphenyl)methylideneamino]guanidine dynamic behaviour. The slight fluctuations reveal the complex systems' conformational stability all through MD simulations. The protein surface area accessed by neighbouring solvent molecules is determined by the Solvent accessible surface area (SASA). When analysing the consistency of proteins throughout MD simulation, the SASA of proteins is further taken into consideration. Figure 5D demonstrates the SASA of the SARS-coronavirus-2 spike protein

over an MD simulation period in both the presence and absence of ligands (2-[(E)-(3-phenylmethoxyphenyl)methylideneamino]guanidine). The SARS-coronavirus-2 spike protein alone and complex were found to have mean SASA values of 10077.67 and 10099.03, respectively. These structures' insignificant SASA variations provide the additional evidence of their stability under physiological conditions. The straight line with negligible fluctuations in all the above mentions parameters demonstrates the system's ultimate success and stayed stable for the simulation duration.

Binding free energy calculations of a top-scoring molecule with SARS-CoV-2 SP target

The MM/GBSA calculation was employed to thoroughly investigate the binding energy needed in the fundamental interaction of both 2-[(E)-(3-phenylmethoxyphenyl)methylideneamino] guanidine with SARS-coronavirus-2 spike glycoprotein enzymes. The MM/GBSA is primarily used to re-evaluate the binding complex's docking conformation and affinities. We examined the impact of the reported ligand on the interaction network with the spike glycoprotein due to the high credibility of this method. To determine the MM/GBSA binding energies, 100 uniformly spaced frames from the entire MD simulation trajectory were taken into account. The various energy components calculated from each entity using the MM/GBSA approach are presented in Table 2. Van der Waals interactions followed by the sum of electrostatic energy and solvation-free energy played a major role in the proposed compounds binding to the spike glycoprotein of SARS-coronavirus-2.

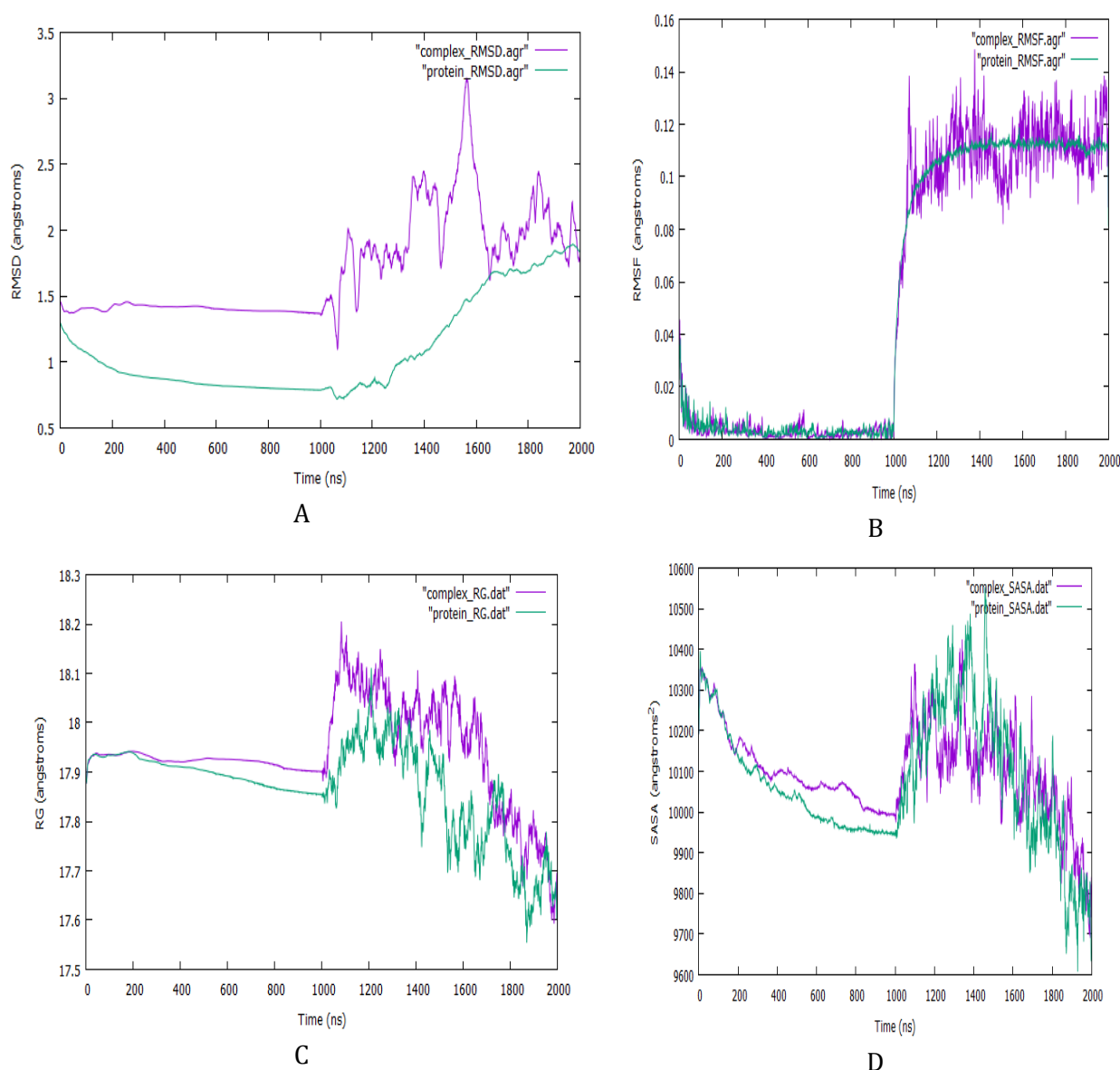


Fig. 5. Assorted pictures of “(A) Root mean square deviation (RMSD), (B) Root mean square fluctuation (RMSF), (C) Radius of gyration (RG), and (D) Solvent accessible surface area (SASA)” for SARS-coronavirus-2 SP (PDB id: 7MZF).

The sum of change in electrostatic and solvation-free energy largely favoured the interaction between the ligand and the spike glycoprotein SARS-CoV-2. The Van der Waals interactions further made a respectable contribution to the overall binding. The complex's overall binding energy was determined to be -86.3641 ± 0.4423 kcal/mol (Table 2).

The physicochemical characteristics of the selected drug compounds are typically related to some search variants when determining how drug-like the substances are. As a result, various drug-likeness rules, including Lipinski's rule [21], Pfizer's rule [22], GSK's rule [23], and the Golden triangle rule [24], were applied to the meaningful physiochemical properties produced from the ADMETlab 2.0 [25] web server (Figure 6).

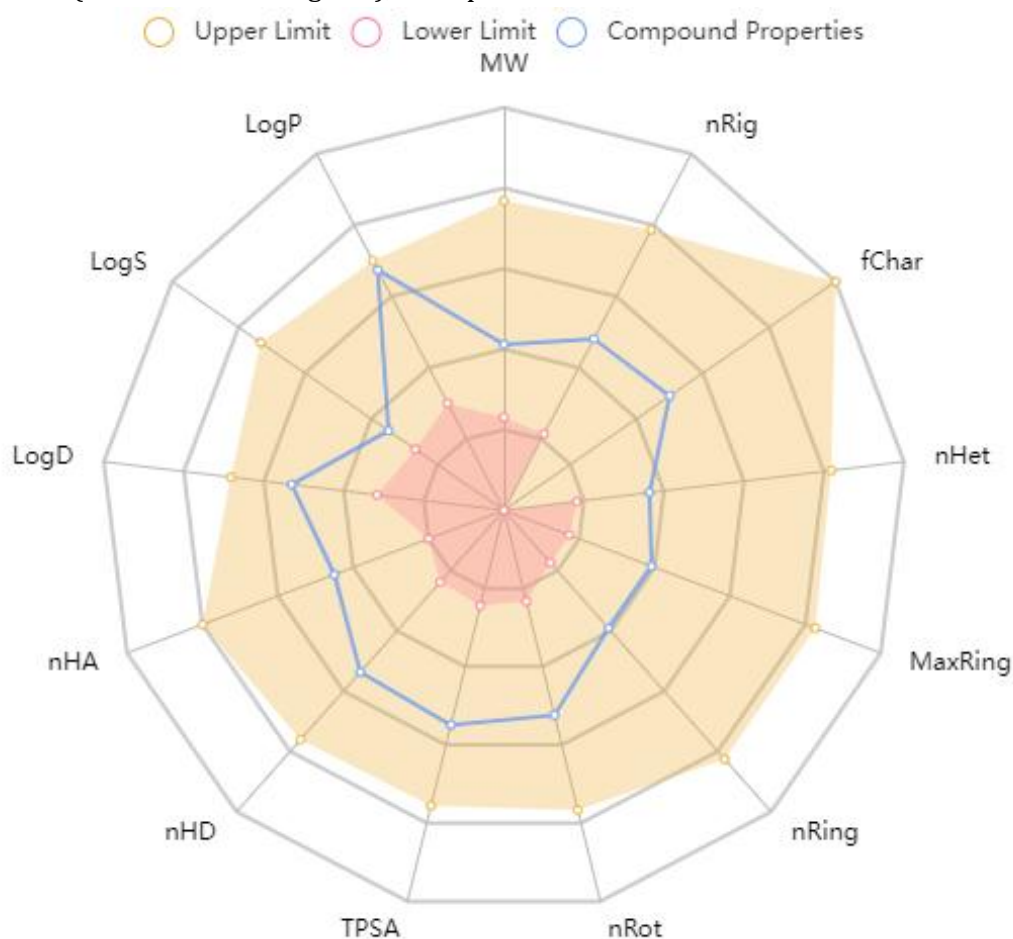
Table 2. MM/GBSA calculation for 2-[(E)-(3-phenylmethoxyphenyl)methylideneamino]guanidine

Parameter	Complex	Protein	Ligand	Total
Ave. BOND	297.6819	290.9191	7.6256	$\delta E_{int} = 1.6227$
Ave. ANGLE	679.5502	677.9823	9.3809	$\delta E_{Elec} + \delta G_{Sol} = -55.9845$
Ave. DIHED	1,796.9034	1,779.6173	6.3565	$\delta E_{VDW} = -32.0023$
Ave. IMPRP	35.8576	36.4654	0.0232	
Ave. ELECT	-5,074.0609	-4,863.4857	-154.5907	$\Delta G_{Binding} = -86.3641 \pm 0.4423 \left(\frac{kcal}{mol}\right)$
Ave. VDW	-611.6909	-604.0992	24.4106	

Key: Ave. = average

Some rules are listed in Table 3. The physicochemical properties for 2-[(E)-(3-phenylmethoxyphenyl)methylideneamino]guanidine and Ruxolitinib are within the upper and lower limit (brown and red regions), as depicted

appropriately in the radar graphs (Figures 6A and 6C). In Figure 6B, Chloroquine fails two of the physicochemical properties, as presented in the radar charts.



A. 2-[(E)-(3-phenylmethoxyphenyl)methylideneamino]guanidine as compound 15

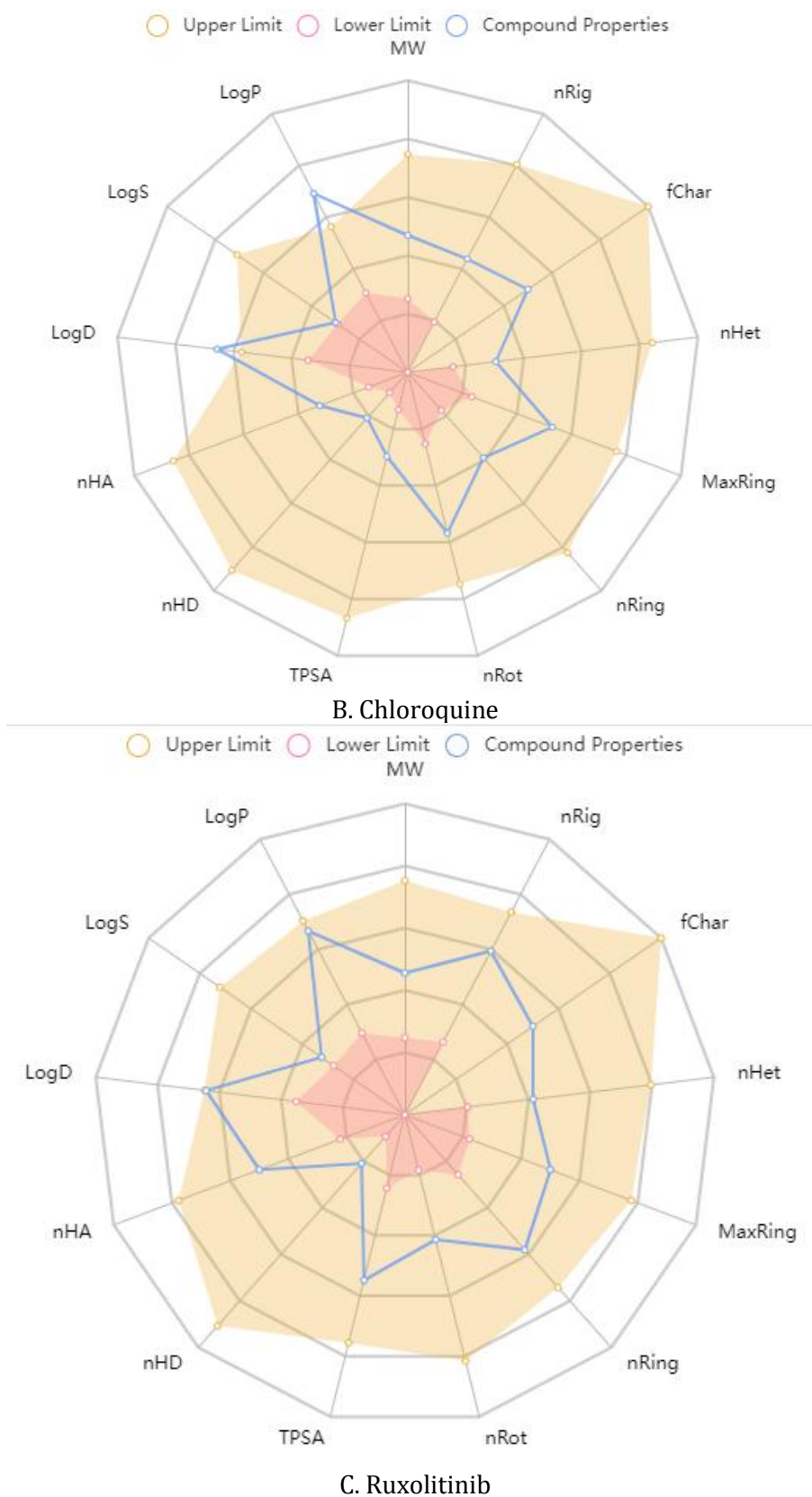


Fig. 6. Physicochemical radar chart of (A) 2-[(E)-(3-phenylmethoxyphenyl)methylideneamino]guanidine, (B) Chloroquine, and (C) Ruxolitinib.

Table 3. Some selected physicochemical properties

Compound name	MW (g/mol)	Log P (log mol/L)	nHA	nHD	Lipinski Rule	Pfizer Rule	GSK Rule	Golden Triangle
Compound 15	268.13	2.802	5	4	Accepted	Accepted	Accepted	Accepted
Chloroquine	319.180	4.511	3	1	Accepted	Accepted	Accepted	Accepted
Ruxolitinib	306.160	2.731	6	1	Accepted	Accepted	Accepted	Accepted

Central: 2-[(E)-(3-phenylmethoxyphenyl)methylideneamino]guanidine (Compound 15) Molecular weight (MW), n-octanol/water distribution coefficient (Log P), number of hydrogens bond acceptors (nHA), number of hydrogen bond donors (nHD).

4- Conclusion

This study used three drugs as SARS-coronavirus-2 spike glycoprotein (SP) inhibitors, using some *in silico* modeling concepts. To conduct a more thorough investigation, the binding affinity against SARS-CoV-2 SP has been calculated using molecular docking. The 2-[(E)-(3-phenylmethoxyphenyl) methylideneamino] guanidine has the most prominent binding affinity score of -7.2 kcal/mol against SARS-coronavirus-2 SP, a magnitude that is significantly more important for being an effective drug when compared with some standard drugs. The accurate binding of 2-[(E)-(3-phenylmethoxyphenyl) methylideneamino] guanidine in SARS-CoV-2 SP via the correct dynamic and energetic changes was confirmed by molecular dynamic simulation studies conducted over 20 ns. In addition, *in silico* ADME studies indicated the general safety and drug-likeness of 2-[(E)-(3-phenylmethoxyphenyl) methylideneamino]guanidine. Therefore, the outcomes of this study provided a solid foundation for the *in silico* plan and hypothetical investigation of SARS-coronavirus-2 inhibitors with increased potency.

Acknowledgements

The authors gratefully acknowledged the technical effort of Adawara Samuel Ndaghiya, Department of Pure and Applied Chemistry, University of Maiduguri, Borno State, Nigeria.

References

- [1] G. A. Heinzl, W. Huang, W. Yu, B. J. Giardina, Y. Zhou, Jr., A. D. MacKerell, A. Wilks, F. Xue, Iminoguanidines as Allosteric Inhibitors of the Iron-Regulated Heme Oxygenase (HemO) of *Pseudomonas aeruginosa*. *Journal of Medicinal Chemistry*, 59 (2016) 6929-6942. <https://doi.org/10.1021/acs.jmedchem.6b00757>
- [2] E. I. Edache, A. Uzairu, P. A. Mamza, G. A. Shallangwa, A 2D-QSAR, Homology Modeling, Docking, ADMET, and Molecular Dynamics Simulations Studies for Assessment of a Novel SARS-Cov-2 and *Pseudomonas Aeruginosa* Inhibitors. *Journal of Virology and Viral Diseases*, 2 (2022) 1-28. <https://doi.org/10.54289/JVVD2200106>.
- [3] E. I. Edache, A. Uzairu, P. A. Mamza, G. A. Shallangwa, QSAR, homology modeling, and docking simulation on SARS- CoV- 2 and *pseudomonas aeruginosa* inhibitors, ADMET, and molecular dynamic simulations to find a possible oral lead candidate. *Journal of Genetic Engineering and Biotechnology*, 20 (2022) 88. <https://doi.org/10.1186/s43141-022-00362-z>.
- [4] R. Custelcean, Iminoguanidines: from anion recognition and separation to carbon capture. *Chemical Communications*, 56 (2020) 10272-10280. <https://doi.org/10.1039/D0CC04332J>.

- [5] Q. Zhang, Y. Jiang, Y. Li, X. Song, X. Luo, Z. Ke, Y. Zou, Design, synthesis, and physicochemical study of a biomass-derived CO₂ sorbent 2,5-furan-bis(iminoguanidine). *iScience*, 24 (2021) 102263.
<https://doi.org/10.1016/j.isci.2021.102263>.
- [6] E. I. Edache, A. Uzairu, P. A. Mamza, G. A. Shallangwa, A comparative QSAR analysis, 3D-QSAR, molecular docking and molecular design of iminoguanidine-based inhibitors of HemO: A rational approach to antibacterial drug design. *Journal of Drugs and Pharmaceutical Science*, 4 (2020) 21-36.
<https://doi.org/10.31248/JDPS2020.036>.
- [7] E. I. Edache, A. Uzairu, P. A. Mamza, G. A. Shallangwa, Theoretical Investigation of the Cooperation of Iminoguanidine with the Enzymes-Binding Domain of Covid-19 and Bacterial Lysozyme Inhibitors and their Pharmacokinetic Properties. *Journal of Mexican Chemical Society*, 66 (2022), 513-542.
<http://dx.doi.org/10.29356/jmcs.v66i4.1726>.
- [8] A. D. Becke, Density-functional thermochemistry. III. The role of exact exchange. *The Journal of Chemical Physics*, 98 (1993) 5648-5652.
<https://doi.org/10.1063/1.464913>.
- [9] C. Lee, W. Yang, R. G. Parr, Development of the Colle-Salvetti correlation-energy formula into a functional of the electron density. *Physical Review B*, 37 (1988) 785-789.
<https://doi.org/10.1103/physrevb.37.785>.
- [10] G. A. Petersson, A. Bennett, T. G. Tensfeldt, M. A. Al-Laham, W. A. Shirley, A complete basis set model chemistry. I. The total energies of closed-shell atoms and hydrides of the first-row elements. *The Journal of Chemical Physics*, 89 (1988) 2193-2218.
<https://doi.org/10.1063/1.455064>.
- [11] M.J. Frisch, G.W. Trucks, H.B. Schlegel, G.E. Scuseria, M.A. Robb, J.R. Cheeseman, G. Scalmani, V. Barone, B. Mennucci, G.A. Petersson, H. Nakatsuji, M. Caricato, X. Li, H.P. Hratchian, A.F. Izmaylov, J. Bloino, G. Zheng, J.L. Sonnenberg, M. Hada, M. Ehara, K. Toyota, R. Fukuda, J. Hasegawa, M. Ishida, T. Nakajima, Y. Honda, O. Kitao, H. Nakai, T. Vreven, J.A. Montgomery, J.E. Peralta, F. Ogliaro, M. Bearpark, J.J. Heyd, E. Brothers, K.N. Kudin, V.N. Staroverov, R. Kobayashi, J. Normand, K. Raghavachari, A. Rendell, J.C. Burant, S.S. Iyengar, J. Tomasi, M. Cossi, N. Rega, J.M. Millam, M. Klene, J.E. Knox, J.B. Cross, V. Bakken, C. Adamo, J. Aramillo, R. Gomperts, R.E. Stratmann, O. Yazyev, A.J. Austin, R. Cammi, C. Pomelli, J.W. Ochterski, R.L. Martin, K. Morokuma, V.G. Zakrzewski, G.A. Voth, P. Salvador, J.J. Dannenberg, S. Dapprich, A.D. Daniels, J.B. Farkas, J.V. Foresman, J. Ortiz, D.J. Cioslowski, Gaussian 09, Revision E. 01, Gaussian, Inc., 2013, Wallingford CT.
- [12] S. Dallakyan, A. J. Olson, Small-molecule library screening by docking with PyRx. *Methods in molecular biology*, 1263 (2015) 243-250.
https://doi.org/10.1007/978-1-4939-2269-7_19.
- [13] M. F. Sanner, Python: a programming language for software integration and development. *Journal of molecular graphics & modelling*, 17 (1999) 57-61.
- [14] J. C. Phillips, D. J. H. Julio D. C. Maia, J. E. Stone, J. V. Ribeiro, R. C. Bernardi, R. Buch, G. Fiorin, J. Henin, W. Jiang, R. McGreevy, M. C. R. Melo, B. K. Radak, R. D. Skeel, A. Singharoy, Y. Wang, B. Roux, A. Aksimentiev, Z. Luthey-Schulten, L. V. Kale, K. Schulten, C. Chipot, E. Tajkhorshid, Scalable molecular dynamics on CPU and GPU architectures with NAMD. *Journal of Chemical Physics*, 153 (2020) 044130;
<https://doi.org/044110.041063/044135.0014475>.
- [15] J. Lee, X. Cheng, J. M. Swails, M. S. Yeom, P. K. Eastman, J. A. Lemkul, S. Wei, J. Buckner, J. C. Jeong, Y. Qi, S. Jo, V. S. Pande, D. A. Case, C. L. Brooks, A. D. MacKerell, Jr, J. B. Klauda, W. Im, CHARMMGUI Input Generator for NAMD, GROMACS, AMBER, Open MM, and

- CHARMM/OpenMM Simulations Using the CHARMM36 Additive Force Field. *Journal of Chemical Theory and Computation*, 12 (2016) 405–413.
<https://doi.org/10.1021/acs.jctc.5b00935>.
- [16] W. Humphrey, A. Dalke, K. Schulten, VMD: visual molecular dynamics. *Journal of molecular graphics*, 14 (1996) 33-38.51.
[https://doi.org/10.1016/0263-7855\(96\)00018-5](https://doi.org/10.1016/0263-7855(96)00018-5).
- [17] E. Wang, H. Sun, J. Wang, Z. Wang, H. Liu, J. Z. H. Zhang, T. Hou, End-point binding free energy calculation with MM/PBSA and MM/GBSA: strategies and applications in drug design. *Chemical Reviews*, 119 (2019) 9478–9508.
<https://doi.org/10.1021/acs.chemrev.9b00055>
- [18] Q. Bai, S. Tan, T. Xu, H. Liu, J. Huang, X. Yao, MolAICal: a soft tool for 3D drug design of protein targets by artificial intelligence and classical algorithm. *Briefings in Bioinformatics*, 22 (2021) bbaa161.
<https://doi.org/10.1093/bib/bbaa161>.
- [19] R. D. Jawarkar, R. L. Bakal, N. Mukherjee, A. Ghosh, M. E. A. Zaki, S. A. AL-Hussain, A. A. Al-Mutairi, A. Samad, A. Gandhi, V. H. Masand, QSAR Evaluations to Unravel the Structural Features in Lysine-Specific Histone Demethylase 1A Inhibitors for Novel Anticancer Lead Development Supported by Molecular Docking, MD Simulation and MMGBSA. *Molecules*, 27 (2022) 4758.
<https://doi.org/10.3390/molecules27154758>.
- [20] F. A. Ugbe, G. A. Shallangwa, A. Uzairu, I. Abdulkadir, Activity modeling, molecular docking and pharmacokinetic studies of some boron-pleuromutilins as anti-wolbachia agents with potential for treatment of filarial diseases. *Chemical Data Collections*, 36 (2021) 100783.
<https://doi.org/10.1016/j.cdc.2021.100783>.
- [21] C. A. Lipinski, F. Lombardo, B. W. Dominy, P. J. Feeney, Experimental and computational approaches to estimate solubility and permeability in drug discovery and development settings. *Advanced Drug Delivery Reviews*, 46 (2001) 3–26.
[https://doi.org/10.1016/s0169-409x\(00\)00129-0](https://doi.org/10.1016/s0169-409x(00)00129-0).
- [22] J. D. Hughes, J. Blagg, D. A. Price, S. Bailey, G. A. Decrescenzo, R. V. Devraj, E. Ellsworth, Y. M. Fobian, M. E. Gibbs, R. W. Gilles, N. Greene, E. Huang, T. Krieger-Burke, J. Loesel, T. Wager, L. Whiteley, Y. Zhang, Physicochemical drug properties associated with in vivo toxicological outcomes. *Bioorganic & medicinal chemistry letters*, 18 (2008) 4872–4875.
<https://doi.org/10.1016/j.bmcl.2008.07.071>.
- [23] Gleeson, M.P. Generation of a set of simple, interpretable ADMET rules of thumb. *Journal of Medicinal Chemistry*, 51(2008) 817–834.
<https://doi.org/10.1021/jm701122q>.
- [24] T. W. Johnson, K. R. Dress, M. Edwards, Using the Golden Triangle to optimize clearance and oral absorption. *Bioorganic & medicinal chemistry letters*, 19 (2009) 5560–5564.
<https://doi.org/10.1016/j.bmcl.2009.08.045>.
- [25] J. Dong, N. N. Wang, Z. J. Yao, L. Zhang, Y. Cheng, D. Ouyang, A. P. Lu, D. S. Cao, ADMETlab: A platform for systematic ADMET evaluation based on a comprehensively collected ADMET database. *J. Cheminform*, 10 (2018) 29.
<https://doi.org/10.1186/s13321-018-0283-x>.

HOW TO CITE THIS ARTICLE

Emmanuel Israel Edache, Adamu Uzairu, Paul Andrew Mamza . Theoretical studies of 2-[(E)-(3-phenylmethoxyphenyl) methylideneamino] guanidine as promising drugs against SARS-coronavirus spike glycoproteins by molecular docking combined with molecular dynamics simulation and MM/GBSA calculation. *Prog. Chem. Biochem. Res*, 6(1) (2023) 46-60.

DOI: 10.22034/pcbr.2023.370115.1237

URL: http://www.pcbiochemres.com/article_167912.html

